Inorganica Chimica Acta 456 (2017) 1–8

Contents lists available at ScienceDirect

Inorganica Chimica Acta

journal homepage: www.elsevier.com/locate/ica

Research paper

A novel compound of triphenyltin(IV) with *N-tert*-butoxycarbonyl-L-ornithine causes cancer cell death by inducing a p53-dependent activation of the mitochondrial pathway of apoptosis

Maria Assunta Girasolo [a,*], Luisa Tesoriere [a], Girolamo Casella [b,e], Alessandro Attanzio [a], Massimo L. Capobianco [c], Piera Sabatino [d], Giampaolo Barone [a,e], Simona Rubino [a], Riccardo Bonsignore [a]

[a] *Dipartimento di Scienze e Tecnologie Biologiche Chimiche e Farmaceutiche (STEBICEF), Università degli Studi di Palermo, Parco d'Orleans II, Viale delle Scienze, Ed.16, 90128 Palermo, Italy*

[b] *Dipartimento di Scienze della Terra e del Mare (DiSTeM), Università degli Studi di Palermo, Via Archirafi 10, 90123 Palermo, Italy*

[c] *ISOF, CNR Area della Ricerca di Bologna, Via P. Gobetti 101, 40129 Bologna, Italy*

[d] *Dipartimento di Chimica "Giacomo Ciamician", Alma Mater Studiorum, Università degli Studi di Bologna, via F. Selmi 2, 40126 Bologna, Italy*

[e] *Consorzio Interuniversitario di Ricerca in Chimica dei Metalli nei Sistemi Biologici (C.I.R.C.M.S.B.) – Piazza Umberto I, 70121 Bari, Italy*

ARTICLE INFO

Article history:
Received 24 July 2016
Received in revised form 7 November 2016
Accepted 11 November 2016
Available online 12 November 2016

Keywords:
Triphenyltin(IV)
Boc-Orn-OH
NMR
Antitumor agents
Apoptosis

ABSTRACT

The triphenyltin(IV) compound with *N-tert*-butoxycarbonyl-L-ornithine (Boc-Orn-OH), [Ph_3Sn(Boc-Orn-O)], was synthesized and characterized by elemental analysis, FT-IR, solution ^{1}H, ^{13}C and ^{119}Sn NMR and ESI mass spectrometry. The organotin(IV) compound inhibited at very low micromolar concentrations the growth of human tumor cell lines HepG2 (hepatocarcinoma cells), MCF-7 (mammary cancer) and HCT116 (colorectal carcinoma) while it did not affect the viability of non-malignant human-derived hepatic cells Chang. The mechanism of the antiproliferative effect of Ph_3Sn(Boc-Orn-O), investigated on human hepatoma HepG2 cells, was pro-apoptotic, being associated with externalization of plasma membrane phosphatidylserine, chromatin condensation or fragmentation and mitochondrial dysfunction as well as with increase of p53 levels.

1. Introduction

Organotin(IV) derivatives have been prepared and tested in the past as possible anticancer agents [1–6] and many of them exhibited interesting activity in specific cancer models. Tin-based drugs represent an excellent alternative to platinum ones as antitumor agents, having the considerable advantage to display a lower toxicity. Triorganotins have demonstrated potential antiproliferative activity *in vitro* [7] against human tumor cell lines, which has been related to their ability to bind to proteins [8,9]. Special attention is given to organotin(IV) carboxylates with significant cytotoxic properties against different cancer cell lines [10,11]. Some compounds have shown strong apoptosis inducing character *in vitro*, which can be higher than the corresponding activity of cisplatin or other clinical anticancer drugs [12].

Although the majority of organotin(IV) compounds cause apoptotic cell death, the exact mechanism of action is not yet clearly determined [13]. Several researches have been focused on understanding the binding mode of organotin(IV) compounds to biologically relevant ligands [3,14], often using small peptides, as low-molecular-weight proteins to mimic the metal ion interaction. The organic ligand facilitates the transport of the compounds across the cell membrane, while the antitumor activity is due to dissociated organotin(IV) moieties.

On account of their structural variability, organotin(IV) derivatives of *N*-substituted amino acids have been extensively studied [14]. Moreover, also organotin(IV) carboxylates of *N*-protected amino acids have shown interesting pharmacological applications as antitumor agents. Thus, it is of particular interest to examine the structural variations caused by protecting groups on the amino nitrogen of the ligand [15]. One of the most widely used *N*-terminal protecting groups is the *tert*-butoxycarbonyl (Boc) group. Boc-amino acids are often used as substrates, substrate analogues or competitive inhibitors of proteolytic enzymes. The study of their conformational preferences is also important for understanding their interactions with enzymes [16].

Several reports have been published concerning structural characterization and bioactivity as antitumor agents of di- and tri-organotin(IV) compounds [17]. Following our previous

* Corresponding author.
E-mail address: assunta.girasolo@unipa.it (M.A. Girasolo).

http://dx.doi.org/10.1016/j.ica.2016.11.012
0020-1693/

investigations on organotin(IV) compounds of L-arginine and *N-tert*-butoxycarbonyl-L-arginine [18,19], we extended our work to the synthesis, structural characterization and biological activity of a triphenyltin(IV) derivative with *N-tert*-butoxycarbonyl-L-ornithine (Boc-Orn-OH) (Fig. 1).

Ph_3Sn(Boc-Orn-O) has been synthesized and characterized by elemental analysis, FT-IR, ESI mass spectrometry, ^1H, ^{13}C and ^{119}Sn NMR spectroscopic techniques and its cytotoxic behavior has been investigated on three human tumor cell lines, HepG2 (hepatocarcinoma cells), MCF-7 (mammary cancer) and HCT116 (colorectal carcinoma) as well as on non-malignant human-derived hepatic cells (Chang). Moreover, the mechanism of its anti-tumor activity has been evaluated.

2. Experimental

2.1. Materials and physical measurements

Ph_3SnOH (Aldrich) and *N-tert*-butoxycarbonyl-L-ornithine (Fluka) were used without further purification. Elemental micro-analyses for C, H and N were performed at the Laboratorio di Microanalisi, University of Padova, Italy. Infrared spectra were recorded with a Perkin-Elmer Spectrum One FT-IR spectrometer, using KBr disc with a resolution of 4 cm^{-1}. All NMR spectra were acquired with an Avance II DMX 400 MHz (9.40 T) spectrometer (Bruker BioSpin GmbH, Rheinstetten, Germany), operating at 400.15 MHz for protons, 100.63 MHz for ^{13}C, and 149.20 MHz for ^{119}Sn. One-dimensional ^1H and $^{13}C\{^1H\}$ spectra in CD_3OD and DMSO-d_6 solutions were acquired at 27 °C with a spectral width (*i.e.* SW) of 12 ppm and 200 ppm, respectively. One-dimensional $^{119}Sn\{^1H\}$ NMR spectra in CD_3OD and DMSO-d_6 solutions were recorded at 27 °C with a SW of 800 ppm by investigating four spectral windows with SW = 250 ppm at once in the +200 to −600 ppm range. For ^{119}Sn, Me_4Sn was employed as external reference (^{119}Sn, δ = 0.00 ppm). ^1H and ^{13}C resonances were calibrated on Me_4Si as external reference (^1H, δ = 0.00 ppm; ^{13}C, δ = 0.00 ppm). $^{119}Sn\{^1H\}$ and $^{13}C\{^1H\}$ spectra were acquired with broadband proton power-gated decoupling. For all nuclei, positive chemical shift had higher frequencies than the reference. LW in the text is intended as line width at half height. Solutions concentrations were ca. $0.5\cdot10^{-3}$ M. Solid-state $^{119}Sn\{^1H\}$ CP-MAS spectra were acquired with NS (*i.e.* number of transients) equal to 1200, using recycling delays of 2 s, contact time of 6 ms and acquisiton time of 11.5 ms. Spinning rates of 5 kHz and 7 kHz were used in order to get the isotropic $\delta^{119}Sn\{^1H\}$value. Line broadening of 75 Hz and zero filling of 16 k points were applied to the free induction decays (FID) before transformation. After calibration on the $(c\text{-}C_6H_{12})_4Sn$, a power level of 4 dB was applied in order to get the Hartman–Hahn condition. 119Sn chemical shifts are given with respect to the solid $(c\text{-}C_6H_{12})_4Sn$ as secondary reference [δ (^{119}Sn) = −97.0 ppm with respect to Me_4Sn]. Solid-state $^{13}C\{^1H\}$ CP-MAS spectra were acquired with NS = 512 using recycling delays of 3 s, contact time of 2 ms and acquisiton time of 34 ms. Spinning rates of 5 kHz and 8 kHz were used in order to get the isotropic $\delta(^{13}C)$ value. Line broadening of 25 Hz and zero filling of 4 k points were applied to the FID before transformation. A power level of 5.1 dB was applied in order to get the Hartman–Hahn condition. ^{13}C chemical shifts are given with respect to the solid admantane as secondary reference [δ ($^{13}CH_2$) = 29.5 ppm; $\delta(^{13}CH)$ = 38.6 ppm with respect to Me_4Si]. Positive-ion and negative-ion electrospray ionization (ESI) mass spectra were measured on an ion trap analyzer Bruker 3000 +in the range *m*/*z* 60–1500. The compound was dissolved in methanol or acetonitrile, diluted at 0.1–1.0 mg/mL in MeOH/H_2O and acetonitrile/H_2O (80/20), and analyzed in ESI-MS by direct infusion at a flow rate of 6 µl/min.

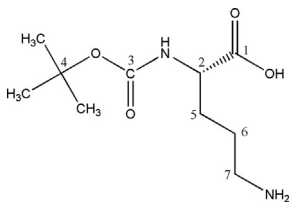

Fig. 1. *N-tert*-butoxycarbonyl-L-ornithine (Boc-Orn-OH).

2.1.1. Synthesis of Ph_3Sn(Boc-Orn-O)

The reaction of Ph_3SnOH with Boc-Orn-OH in a 1:1 molar ratio, led to the formation of the organotin(IV) compound according to Eq. (1)

$$Ph_3SnOH + \text{Boc-Orn-OH} \rightarrow Ph_3Sn(\text{Boc-Orn-O}) + H_2O \quad (1)$$

A solution of Ph_3SnOH (0.734 g, 2 mmol) in dry methanol (15 mL) was added drop wise to a methanol solution (15 mL) of the ligand (Boc-Orn-OH, 0.464 g, 2 mmol) and left to react, under stirring, for 4 h. After cooling at room temperature, the solvent was reduced under *vacuum* to a small volume (5 mL) using a rotary evaporator; a white solid residual was obtained, which was filtered off, washed three times with a total amount of methanol of 50 mL and dried *in vacuo* in presence of P_4O_{10}. $C_{28}H_{34}N_2O_4Sn$: *M* = 581.31 g/mol; m.p. = 118 °C; Anal.Calc.: C 57.85, H 5.89, N 4.82, Sn 20.42%. Found: C 57.50, H 6.16, N 5.11, Sn 20.31%. IR (KBr, cm^{-1}): 3379 m, 3327w, 3263 m ν(NH); 1654 s $\nu_{as}(COO^-)$, 1413 m $\nu_s(COO^-)$, $\Delta\nu$ = 241; 280 m ν_{as}(sn-C), 227w ν_s(sn-C). ^1H NMR (400.15 MHz, CD_3OD): δ (ppm) 7.78–7.76 (br, 6H, *o*-protons in $SnPh_3$, $|^3J(^{119}Sn,^1H)|$ = 59.0 Hz); 7.49–7.42 (br, m, 9H, *m*- and *p*-protons in $SnPh_3$); 3.93 (br,1H, H-2); 2.88 (t, 2H, H-7); 1.81(m, 2H, H-5); 1.66 (m, 2H, H-6); 1.41 (s, 9H, Boc). ^{13}C NMR (100.63 MHz, CD_3OD): δ (ppm) 173.4 (C-1); 157.6–158.2 (C-3); 140.8–140.9 (Sn–C_6H_5 *ipso*, $^1J(^{119}Sn,^{13}C)|$ = 738 Hz); 137.7 (Sn–C_6H_5 *ortho*, $|^2J(^{119}Sn,C)|$ = 43.2 Hz); 129.7 (Sn–C_6H_5 *meta*, $|^3J(^{119}Sn,C)|$ = 64.4 Hz); 130.5–130.6 (Sn–C_6H_5 *para*, $|^4J(^{119}Sn,C)|$ = 13.4 Hz); 80.3 (C_{quat}-4); 52.5 (C-2); 42.7 (C-7); 29.3 (C-5); 28.8 (C-Boc); 22.3 (C-6). ^{119}Sn NMR (149.20 MHz, CD_3OD): δ (ppm) −166.8. ^1H NMR (400.15 MHz, DMSO-d_6): δ (ppm) 7.79–7.78 (d, 6H, *o*-protons in $SnPh_3$, $|^3J(^{119}Sn,C)|$ = 59.5 Hz); 7.40–7.38 (d, 9H, *m*- and *p*-protons in $SnPh_3$); 3.70 (d, 1H, H-2); 2.39 (t, 2H, H-7); 1.92–1.74 (m, 2H, H-5), 1.51 (d, 2H, H-6), 1.38 (s, 9H, Boc). ^{13}C NMR (100.63 MHz, DMSO-d_6): δ (ppm) 170.1 (C-1); 155.3 (C-3); 142.5–141.9 (Sn–C_6H_5 *ipso*); 136.1–135.9 (Sn–C_6H_5 *ortho*), $^2J(^{119}Sn,C)|$ = 42.4 Hz; 128.2 (Sn–C_6H_5 *meta*, $|^3J(^{119}Sn,C)|$ = 59.5 Hz; 128.9 (Sn–C_6H_5 *para*); 77.6 (C_{quat}-4); 50.2 (C-2); 40.9 (C-7); 28.2 (C-Boc); 27.8 (C-5); 21.1 (C-6). ^{119}Sn NMR (149.20 MHz, DMSO-d_6): δ (ppm) −125.9, −137.5. CP-MAS ^{13}C NMR (100.63 MHz) for the ligand: δ (ppm) 179.1 (C-1); 156.5 (C-3); 77.6 (C_{quat}-4); 58.5 (C-2); 40.7 (C-7); 30.9 (C-Boc); 29.2 (C-5); 25.4 (C-6); CP-MAS ^{13}C NMR (100.63 MHz) for the compound: δ (ppm) 179.5, 176.1, 171.8 (C-1); 157.4 (C-3); 146.8 (Sn–C_6H_5 *ipso*); 143.0 (Sn–C_6H_5 *ortho*); 128.6 (Sn–C_6H_5 *meta*); 137.8, 134.5 (Sn–C_6H_5 *para*); 77.2 (C_{quat}-4); 58.4, 52.9, 50.4 (C-2); 42.3, 40.7, 38.5 (C-7); 29.6 (C-Boc); 24.5 (C-5); 22.0 (C-6); CP-MAS ^{119}Sn NMR (149.20 MHz): δ (ppm) -297. ESI-MS: M_W = 582. Positive-ion MS: *m*/*z* 604.9 [M + Na]$^+$; *m*/*z* 582.9 [M + H]$^+$; Negative-ion MS: *m*/*z* 626.8 [M + HCOO]$^-$; *m*/*z* 580.9 [M-H]$^-$ traces.

Due to the low solubility of the ligand, $^{13}C\{^1H\}$ NMR spectra of Boc-Orn-OH and Ph_3Sn(Boc-Orn-O), were recorded also in solid state to check the compound formation.

2.2. Biological assays

2.2.1. Viability assay in vitro

Ph_3Sn(Boc-Orn-O) was dissolved in dimethyl sulfoxide (DMSO) and then diluted in culture medium so that the effective DMSO concentration did not exceed 0.1%. HepG2, MCF-7 and HCT116 tumor cell lines and human hepatic Chang liver cells were purchased from American Type Culture Collection, Rockville, MD, USA. All of them were grown in RPMI medium supplemented with L-glutamine (2 mM), 10% fetal bovine serum (FBS), penicillin (100 U/mL), streptomycin (100 μg/mL) and gentamicin (5 μg/mL). HepG2 culture medium also contained sodium pyruvate (1.0 mM). Cells were maintained in log phase by seeding twice a week at a density of 3×10^8 cells/L in humidified 5% CO_2 atmosphere, at 37 °C. In all experiments, cells were made quiescent through overnight incubation before the treatment with the compounds or vehicle alone (control cells). No differences were found between cells treated with DMSO 0.1% and untreated cells in terms of cell number and viability.

Cytotoxic activity of Ph_3Sn(Boc-Orn-O) against three human tumor cell lines HepG2, MCF-7, HCT116 and human hepatic Chang liver cells was determined by the MTT colorimetric assay based on the reduction of 3-(4,5-dimethyl-2-thiazolyl)bromide-2,5-diphenyl-2H-tetrazolium (MTT) [20] to purple formazan by mitochondrial dehydrogenases of living cells. This method is commonly used to illustrate inhibition of cellular proliferation. Monolayer cultures were treated for 24 h with various concentrations (0.1–5 μM) of the drug. Cisplatin was used for comparison.

Briefly, all cell lines cells were seeded at 2×10^4 cells/well in 96-well plates containing 200 μL RPMI. After an overnight incubation, cells were washed with fresh medium and incubated with the compounds in RPMI. After 24 h incubation, cells were washed, and 50 μL FBS-free medium containing 5 mg/mL MTT were added. The medium was discarded after 2 h incubation at 37 °C by centrifugation, and formazan blue formed in the cells was dissolved in DMSO. The absorbance, measured at 570 nm in a microplate reader (Bio-RAD, Hercules, CA), of MTT concentration at which 50% of cells remained viable relative to the control. Each experiment was repeated at least three times in triplicate to obtain the mean values.

2.2.2. Measurement of phosphatidylserine exposure

HepG2 cells were seeded in triplicate in 24-wells culture plates at a density of 5.0×10^4 cells/cm^2. After overnight incubation, the cells were washed with fresh medium and incubated with the 1–2 μM compound in RPMI. After 24 h, cells were harvested by trypsinization, collected by centrifugation and submitted to Annexin V-FITC/PI double staining (eBioscience, San Diego, CA) as reported [19]. Samples of at least 1.0×10^4 cells were analyzed by fluorescence-activated cell sorting (FACS) analysis by Epics XL™ flow cytometer using Expo32 software (Beckman Coulter, Fullerton, CA), using appropriate 2-bidimensional gating method.

2.2.3. Acridine orange and ethidium bromide morphological fluorescence dye staining

Dual staining with acridine orange (AO)/ethidium bromide (EB) allows enumeration of populations of viable non apoptotic, viable (early) apoptotic, nonviable (late) apoptotic, and necrotic cells [21]. Briefly, after HepG2 cells were treated with Ph_3Sn(Boc-Orn-O) at 1–2 μM concentration for 24 h, the medium was discarded. Cells were washed with saline 5 mM phosphate buffer (PBS) and then incubated with 100 μL PBS containing 100 μg/mL of EB plus 100 μg/mL of AO. After 20 s, EB/AO solution was discarded and cells immediately visualized by means of fluorescent microscope equipped with an automatic photomicrograph system (Leica, Wetzlar, Germany). Multiple photos were taken at randomly selected areas of the well to ensure that the data obtained are representative.

2.2.4. Measurement of mitochondrial transmembrane potential

Mitochondrial transmembrane potential ($\Delta\psi m$) was assayed by flow cytofluorometry, using the cationic lipophilic dye 3,30-dihexyloxacarbocyanine iodide [$DiOC_6(3)$] (Molecular Probes,Inc.) which accumulates in the mitochondrial matrix. Changes in mitochondrial membrane potential are indicated by a reduction in the DiOC6-induced fluorescence intensity. Cells were incubated with $DiOC_6(3)$ at a 40 nmol/L final concentration, for 15 min at 37 °C. After centrifugation, cells were washed with PBS and suspended in 500 μL PBS. Samples of at least 1×10^4 cells for each sample were subjected to FACS analysis by Epics XL™ flow cytometer as above reported.

2.2.5. Measurement of cytosolic calcium

Intracellular Ca^{2+} concentration in a single cell was measured using fluo-3/AM as a fluorescent Ca^{2+} probe, whose intensity is directly representative of cellular concentration of the ion. Fluo-3/AM, at 2 mM final concentration, was added into the cell medium 40 min before the end of the treatment. After centrifugation, cells were washed with PBS and suspended in 500 μL PBS. The fluorescent intensities were analyzed by fluorescence-activated cell sorting analysis in at least $1x10^4$ cells for each sample.

2.2.6. Measurement of intracellular reactive oxygen species (ROS)

ROS level was monitored by measuring fluorescence changes that resulted from intracellular oxidation of dichloro-dihydro-fluorescein-diacetate (DCFH-DA). DCFH-DA, at 10 mM final concentration, was added to the cell medium 30 min before the end of the treatment. The cells were collected by centrifugation for 5 min at 2000 rpm at 4 °C, washed, suspended in PBS and immediately subjected to fluorescence-activated cell sorting analysis. At least 1×10^4 cells were analyzed for each sample.

2.2.7. Western blot analysis

After treatment with the compound, protein extracts were prepared and equal amounts of protein samples (80 μg/lane), subjected to SDS-PAGE and transferred to nitrocellulose membrane as previously reported [21]. The immunoblot was incubated overnight at 4 °C with blocking solution (5% skim milk), followed by incubation with anti-PARP monoclonal antibody (clone D-1, Cat No. SC-365315, Santa Cruz Biotechnology, Santa Cruz, CA), or anti-p53 (FL-393, Cat No SC-6243, Santa Cruz Biotechnology) for 1 h at room temperature. Blots were washed two times with Tween 20/Tris-buffered saline (TTBS) and incubated with a 1:2000 dilution of horseradish peroxidase (HRP)-conjugated anti-IgG antibody (Dako Denmark, Glostrup, Denmark) for 1 h at room temperature. Blots were again washed five times with TTBS and then developed by enhanced chemiluminescence (Amersham Life Science, Arlington Heights, IL, U.S.A.). Immunoreactions were also performed using β-actin antibody as loading controls.

2.2.8. Statistical analysis

Results are given as mean ± SD. Three independent observations were carried out for each experiment replicated three times. Comparison between matched-paired samples was by Student's *t* test. In all cases, significance was accepted if the null hypothesis was rejected at the $P < 0.05$ level.

3. Results and discussion

3.1. Spectroscopic data

The IR bands of compound were assigned by comparison with the IR spectra of the free amino acid (*N-tert*-butoxycarbonyl-L-

ornithine) [22,23] and of the related organotin(IV) compound (Ph_3-SnOH). The vibration at 3379 cm^{-1} in the IR spectra of the ligand attributed to the ν(N–H), remains unaltered in the compound. Ph_3-SnOH exhibits a ν(OH) absorption band of medium intensity at 3617 cm^{-1}, which is not observed in the Ph_3Sn(Boc-Orn-O) due to the loss of the OH group on binding to the ligand. The infrared spectrum of the free ligand shows a band at ca. 1631 cm^{-1} corresponding to the vibrational stretching mode $\nu_{asym}(COO^-)$ of the carboxylate moiety. After deprotonation and binding to tin atom, this band is replaced by a strong absorption at 1654 cm^{-1}, while the corresponding $\nu_s(COO^-)$ at 1413 cm^{-1} remains unshifted. The considerable shift of the $\nu_{asym}(COO^-)$ vibration upon coordination in Ph_3Sn(Boc-Orn-O) is due to the binding to the metal through the carboxyl oxygen atom. The criterion of the separation between the symmetric and asymmetric stretching wavenumbers of the carboxylate moiety, $\Delta\nu = [\nu(COO^-)_{asym} - \nu(COO^-)_{sym}]$, has been applied to ascertain its bidentate/chelation or monodentate coordination type [24]. Although a clear line between the two categories cannot be drawn, the observed value of $\Delta\nu$ (241 cm^{-1}) strongly points to a monodentate coordination of the carboxylate group of the ligand to the tin atom [25]. For a bridging or chelating carboxylate group, $\Delta\nu$ would be expected to be <150 cm^{-1}, as widely observed in the infrared spectra of triorganotin(IV) carboxylates [26]. A medium intensity band corresponding to the sn-O stretching mode of vibration appears at 447 cm^{-1}, while the bands at 280 and 227 cm^{-1} are attributed to ν_{as}(sn-C) and ν_s(sn-C) stretching modes, respectively. Thus, the presence of both asymmetric and symmetric stretching vibrations in the infrared spectra of the compound in the solid state rules out planar arrangement of the three sn-Ph bonds. The appearance of two new bands of strong intensity in the IR spectra of Ph_3Sn(Boc-Orn-O) at 693 and 722 cm^{-1} may be assigned to the C-H out-of-plane deformation vibrations [27]. The compound also shows the characteristic Whiffen Y-mode absorption at 450 cm^{-1}, typical of the covalent phenyl-tin bonds [28].

The measured ^1H, ^{13}C and ^{119}Sn chemical shifts, in ppm, in CD_3OD and DMSO-d_6 solutions, are given in the experimental section. ^{13}C NMR resonances for the free ligand in solution could not be recorded due to its limited solubility. The resonances for the organotin(IV) compound are compared with the free ligand L-ornithine [29]. In the ^1H NMR spectra of Ph_3Sn(Boc-Orn-O), proton resonances experience a shift towards higher frequencies for H-5, H-6 and H-7, while H-2 and Boc's protons remain almost unchanged. The resonances ascribed to the aromatic protons of the phenyl groups, appeared as two well separated sets of multiplets in the regions centered around 7.78 and 7.42 ppm in CD_3OD, and 7.79 and 7.38 in DMSO-d_6. In addition to these signals, ^1H NMR spectra of Ph_3Sn(Boc-Orn-O) showed one signal at 1.41 ppm in CD_3OD and 1.38 ppm in DMSO-d_6, corresponding to the protons of the Boc group. The signal of the carboxylic carbon (C-1) is observed at 173.4 ppm in CD_3OD and 170.1 ppm in DMSO-d_6 solutions. Ph_3Sn (Boc-Orn-O) exhibits the signals of the *ipso*-carbon atoms of the phenyl ring at 140.8 and 140.9 ppm in CD_3OD, while in DMSO-d_6 these signals are found at 142.05 and 141.98 ppm: the presence of these two peaks also indicate two different symmetries around the central Sn atom. In CD_3OD, the $^1J(^{119}Sn,^{13}C)$ value of 738 Hz, is closer to the low limit of the typical $^1J(^{119}Sn,^{13}C)$ range (750–850 Hz) [30–32] for penta-coordinated triphenyltin(IV) compounds rather than to the range (550–650 Hz) of tetra-coordinated ones. In CD_3OD solution, the measured ^{119}Sn chemical shift of -166.8 ppm (LW = 380 Hz) for organotin(IV) compound, lies at the boundary between tetra- and penta-coordinated tin [30,18], even if it is more shifted towards a penta-coordinated tin arrangement. In addition, the large measured LW for the tin signal indicates the occurrence of a dynamic process conceivably due to solvent-tin exchange. In order to check the effect of the solvent upon the $\delta(^{119}Sn)$, a further ^{119}Sn NMR spectrum has been acquired in DMSO-d_6 solution. Two signals, with LW values smaller than in methanol solution, were found at -125.3 (LW ≅ 120 Hz) and −137.0 ppm (LW ≅ 120 Hz), again pointing to penta-coordination on the tin center. The two similar $\delta(^{119}Sn)$ values indicate a slight symmetry variation around the tin center. Moreover, despite the greater coordinating ability of DMSO-d_6 relative to CD_3OD, in DMSO-d_6 the observed signals were more deshielded than in CD_3OD solution, most likely due to the occurrence of weaker sn—DMSO interaction. These findings highlight the existence of

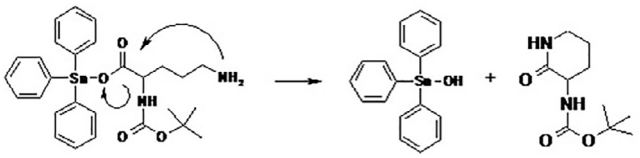

Scheme 1. Speculative origin of the fragment $C_{10}H_{18}N_2O_3$.

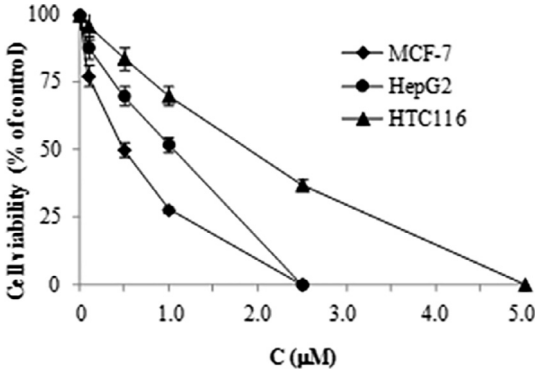

Fig. 2. Effect of Ph_3Sn(Boc-Orn-O) on survival of different human tumor cell lines. Cells were treated with the test compound and cell survival was measured after 24 h by MTT assay in comparison to cells treated with vehicle alone (control).

Table 1
IC_{50} values (μM) for the *in vitro* anti-proliferative activity of triphenyltin(IV) compound and cisplatin, determined by MTT test, on different human tumor cell lines.

Compound	MCF-7	IC_{50} ± SD	
		HepG2	HTC116
Ph_3Sn(Boc-Orn-O)	0.52 ± 0.04	1.08 ± 0.09	2.24 ± 0.18
Cisplatin	11.2 ± 1.5	64.3 ± 4.3	46.5 ± 3.5

Values are the mean ± SD of three separate experiments in triplicate.

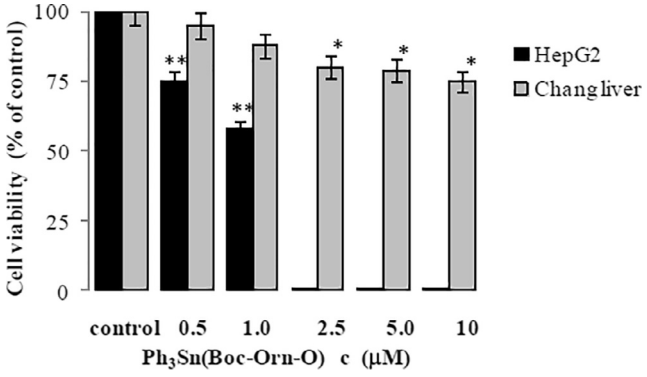

Fig. 3. Cytotoxicity of Ph_3Sn(Boc-Orn-O) on HepG2 tumor liver cells in comparison with non-malignant human-derived hepatic cells Chang. Cells were treated with the test compound and cell survival was measured after 24 h by MTT assay in comparison to cells treated with vehicle alone (control). With respect to control, values were significant with *P < 0.05 or **P < 0.0001 (Student's *t*-test).

monomeric units of the compound in both solution phases where the metal center is also involved in tin-solvent exchange.

In order to distinguish between the spectroscopic data relating to a monomeric or to a long-chain polymeric structure, the mass spectral data for the organotin(IV) compound were recorded. Tin-containing ions are known to form dimeric and polymeric species [33] and indeed dimeric ions and adducts with sodium and hydrogen were found. All the ions containing tin were observed with the expected isotopic distribution and the given attributions were done after comparison with the simulated spectra obtained by the native software of our instrument. In the positive mode, all the ions can be related with the mass of our compound M or with the dimeric cluster 2 M and fragmentations from these species. All the principal ions found can be attributed as follows: *m/z* 1185.0 and 1163.0 $[2\,M + Na]^+$ and $[2\,M + H]^+$ respectively; *m/z* 953.0 and 931.0 $[M\text{-}H + Ph_3Sn + Na]^+$ and $[M + Ph_3Sn]^+$ respectively; *m/z* 819.0 $[M + C_{10}H_{18}N_2O_3 + Na]^+$; *m/z* 716.8 $[(Ph_3Sn)_2O + H]^+$ found also by others [34]; *m/z* 604.9 and 582.9 $[M + Na]^+$ and $[M + H]^+$ respectively; *m/z* 450.9 $[2C_{10}H_{18}N_2O_3 + Na]^+$; *m/z* 236.9 $[C_{10}H_{18}N_2O_3 + Na]^+$, where the C_{10} residue could be originated from the fragmention of Ph_3Sn(Boc-Orn-O) according to Scheme 1. It is worthy to note that no peaks derived from the free Boc-Orn-OH were detected, and that the C_{10} residue found in the analysis of Ph_3Sn(Boc-Orn-O) was not observed during the analysis of the free Boc-Orn-OH in similar conditions. Our organotin(IV) compound was also investigated applying a negative voltage, again revealing ions originated from the presumed structure as deprotonated species or as adducts with formiate such as: *m/z* 812.9 $[M + BocOrn\text{-}O]^-$, *m/z* 760.7 $[(Ph_3Sn)_2O + HCOO]^-$; *m/z* 626.8 $[M + HCOO]^-$, *m/z* 580.9 $[M\text{-}H]^-$ only present in traces, and *m/z* 231.1 $[Boc\text{-}Orn\text{-}O]^-$.

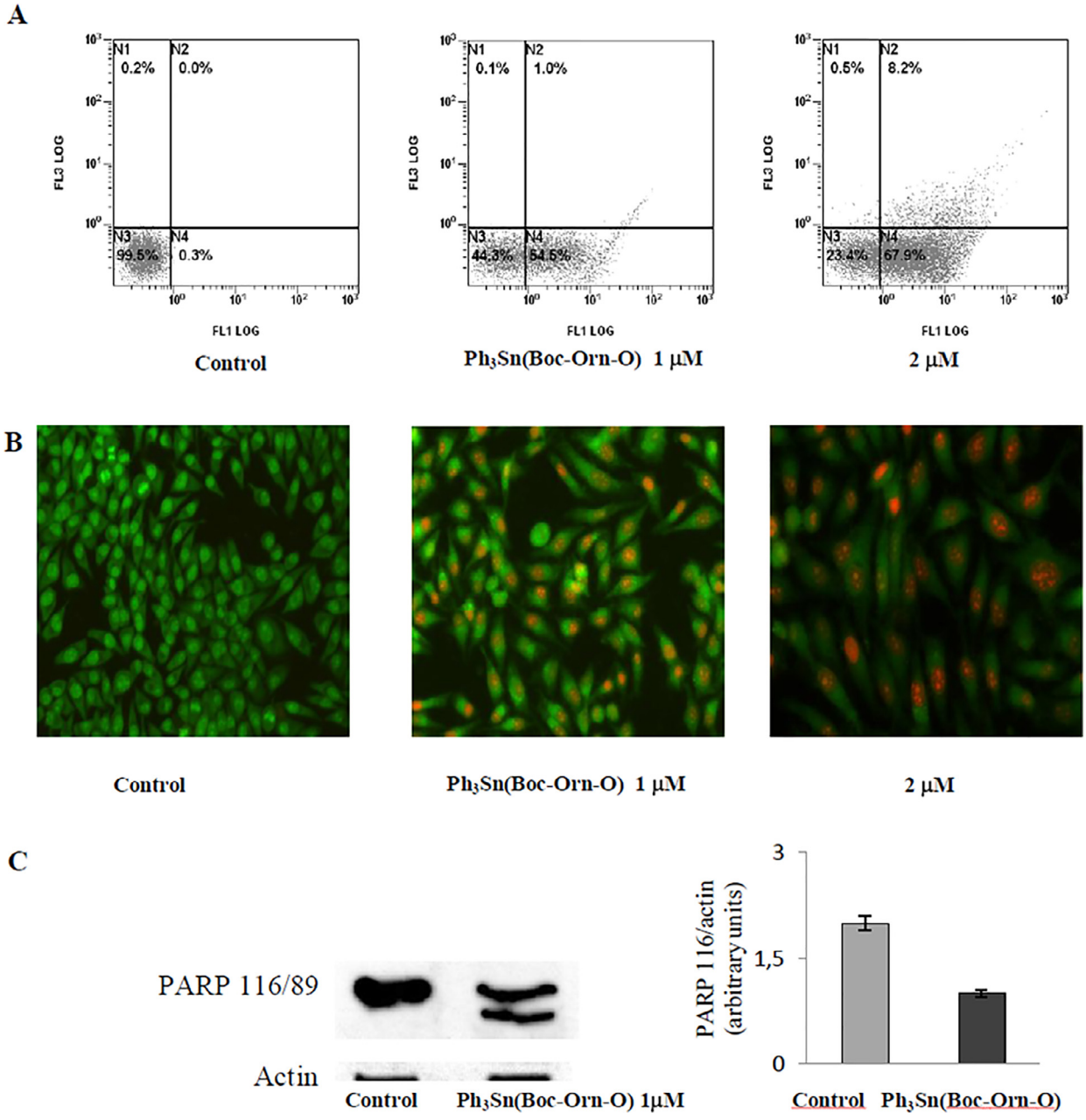

Fig. 4. Ph_3Sn(Boc-Orn-O) induces dose-dependent apoptosis in HepG2 cells. (A) Percentage of Annexin V/propidium iodide (PI) double-stained HepG2 cells, as determined by flow cytometry. (B) Fluorescence micrographs of ethidium bromide/acridine orange double-stained HepG2 cells in 200× magnification. (C) Poly(ADP-ribose) polymerase cleavage by immunoblotting with densitometric analysis of the immunoblots. Data of the densitometric analysis are means and standard deviations. Control, cells treated with vehicle. Representative images of three experiments with comparable results.

3.2. Biological results

3.2.1. Cytotoxic activity

The *in vitro* cytotoxicity of Ph_3Sn(Boc-Orn-O) against human tumor cell lines HepG2, HTC116 and MCF-7 was evaluated using MTT metabolic assay. After 24 h of incubation, a dose dependent antiproliferative effect at very low micromolar concentrations of the compound toward all the studied cancer cell lines was measured (Fig. 2). Table 1 reports the concentration of Ph_3Sn(Boc-Orn-O) required to inhibit 50% of cell proliferation when compared to untreated cells (IC_{50}).

In addition, cytotoxicity of cisplatin, one of the most widely used antitumor drugs in clinical practice, has been included. On direct comparison with cisplatin, the antiproliferative activity of synthesized organotin(IV) derivative is from 20 to 60 times stronger, being the highest triphenyltin(IV) compound/cisplatin activity ratio observed, under the investigated conditions, in the HepG2 cells.

In order to determine the selectivity in the *in vitro* cytotoxicity of organotin(IV) compound, some additional experiments were conducted on non-malignant human-derived hepatic cells Chang. As shown in Fig. 3, at the concentrations effective to totally inhibit the growth of HepG2 liver tumor cells, Ph_3Sn(Boc-Orn-O) shows only a modest effect on the viability of normal-like Chang cells, indicating selectivity towards cancer cells.

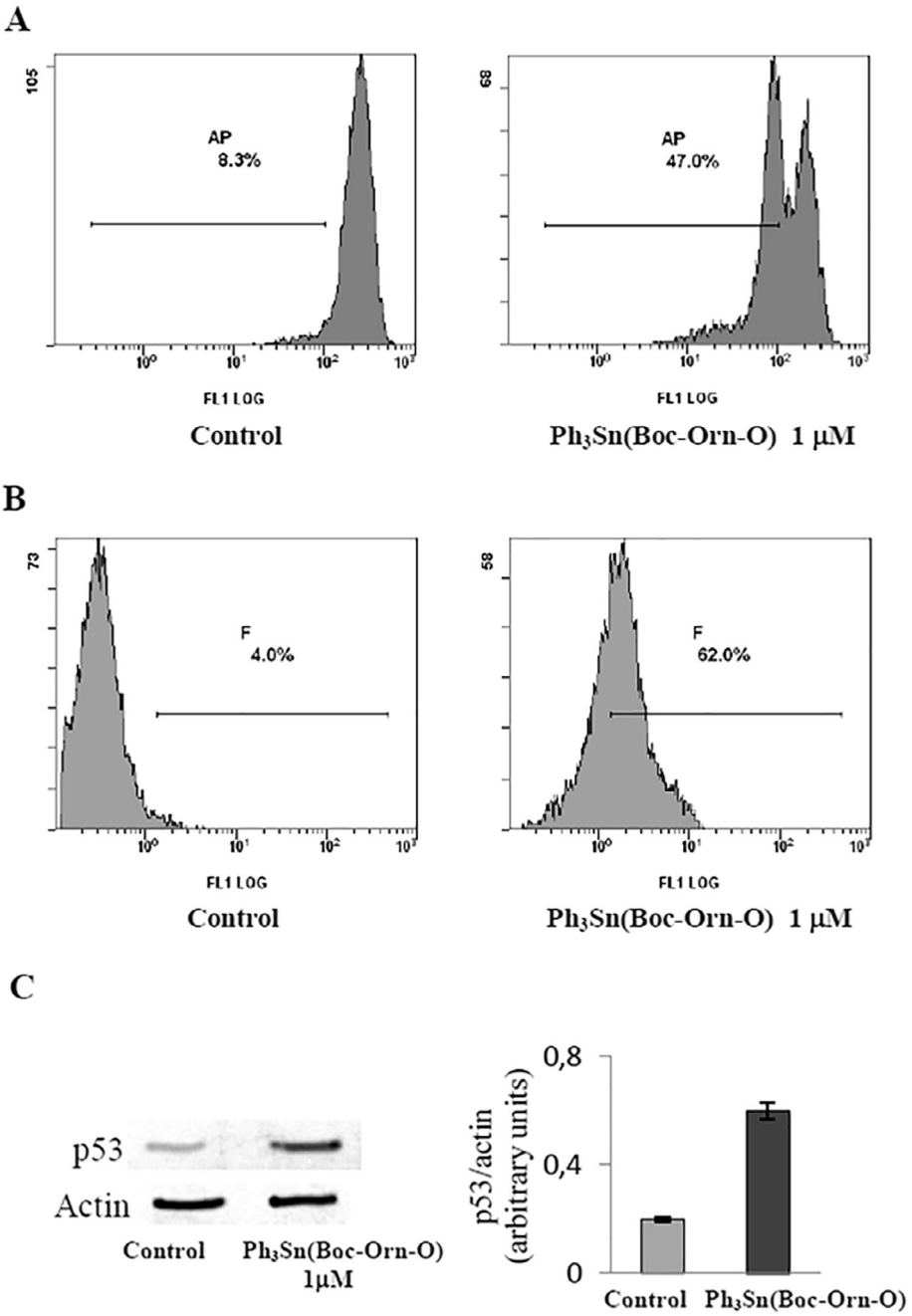

Fig. 5. Effects of Ph_3Sn(Boc-Orn-O) on the activation of mitochondrial dysfunction in HepG2 cells. (A) The $\Delta\psi m$ was detected by fluorescence intensity of 3,30-dihexyloxacarbocyanine iodide-treated cells, as determined by flow cytometry. (B) Ca^{2+} levels were assayed after cell loading with fluo-3/AM followed by flow cytometry analysis. (C) p53 level by immunoblotting with densitometric analysis of the immunoblots. Data of the densitometric analysis are means and standard deviations. Control, cells treated with vehicle. Representative images of three experiments with comparable results.

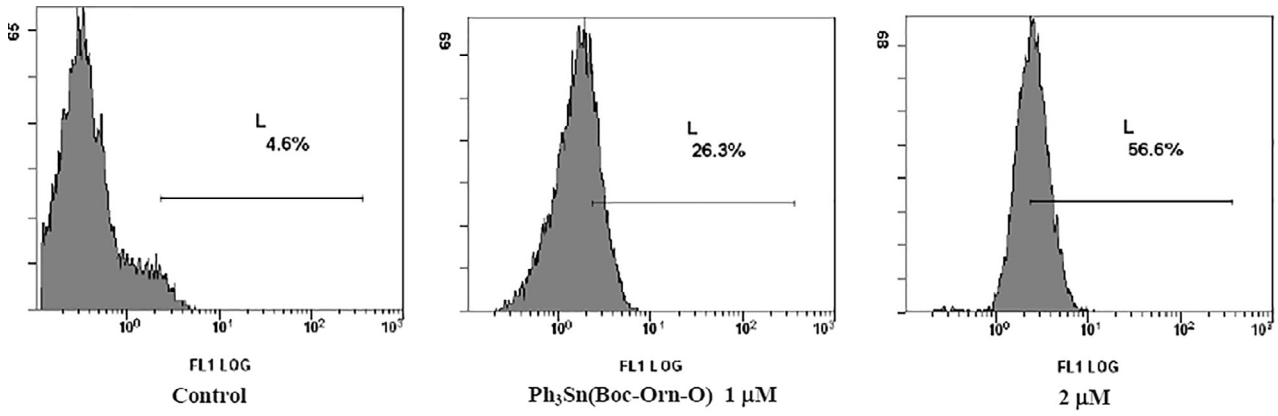

Fig. 6. Ph_3Sn(Boc-Orn-O) caused dose-dependent ROS production in HepG2 cells. ROS were detected by fluorescence intensity of 2′,7′-dichlorofluorescin diacetate-treated cells, as determined by flow cytometry. Control, cells treated with vehicle. Representative images of three experiments with comparable results.

3.2.2. Induction of apoptosis in HepG2 cells

To determine whether the antiproliferative effect of Ph_3Sn(Boc-Orn-O) was due to apoptosis, HepG2 cells were treated with the compound for 24 h, stained with both propidium iodide (PI) and Annexin V-fluorescein isothiocyanate (FITC), and analyzed by flow cytometry. The chosen concentrations were selected on the basis that they represented IC_{50} and twice the IC_{50} value. As shown in Fig. 4A, the control cells stained negative for both Annexin V-FITC and PI. On the other hand, HepG2 cells treated with increasing doses, showed increased proportions of Annexin V-positive cells, indicating that they were at an early stage of apoptosis. The double positive staining of particular cells also increased, which revealed that these cells were at a late apoptotic stage. To confirm apoptotic mechanism of cytotoxicity of Ph_3Sn(Boc-Orn-O), we carried out morphological evaluation of HepG2 cells using AO and EB double staining. After 24 h of treatment with 1 μM of Ph_3Sn(Boc-Orn-O), fluorescent microscopy revealed the appearance of cells containing bright green patches in the nuclei as a consequence of chromatin condensation and nuclear fragmentation, which are typical features of apoptosis. Moreover, after treatment with the compound at 2 μM concentration, fluorescing orange cells owing to increase of cell permeability to ethidium bromide, cell shrinkage and nuclear fragmentation were also evident as observed for cells in late apoptosis (Fig. 4B).

One of the key executioners of the apoptotic cell death is caspase 3, responsible for proteolytic cleavage of many key proteins, including poly(ADP-ribose) polymerase-1 (PARP-1). In comparison with control cells, high levels of the 89 kD cleaved product from PARP-1, with a decrease of the 116 kD native protein, were observed in HepG2 cells after 24 treatment with Ph_3Sn(Boc-Orn-O) (Fig. 4C). Taken together, these findings provided strong evidence that the synthesized Ph_3Sn(Boc-Orn-O) induced apoptosis in HepG2 cells.

3.2.3. Mitochondrial damage

In many systems, apoptosis is associated with the loss of mitochondrial inner membrane potential ($\Delta\psi m$) which is responsible for the release of some pro-apoptotic factors from the organelle. We investigated the involvement of mitochondria in apoptosis induced by the tin compound using $DiOC_6(3)$, a fluorescent mitochondria-specific and voltage-dependent dye. The results, reported in Fig. 5A, indicate that treatment of HepG2 cells with 1 μM of Ph_3Sn(Boc-Orn-O) for 24 h, induced a marked dissipation of $\Delta\psi m$ as indicated by decreased mitochondrial DiOC6-red.

Owing to mitochondrial dysfunction, perturbation of the intracellular calcium level is expected. A Fluo-3/AM staining followed by flow cytometry analysis, gave evidences that, in comparison with control cells, treatment of HepG2 cells with Ph_3Sn(Boc-Orn-O) also caused a net elevation of cellular Ca^{2+} content, evident by the increment of fluorescence of the ion probe (Fig. 5B).

To understand more about the apoptosis induction mechanism caused by Ph_3Sn(Boc-Orn-O), the levels of p53 protein was assessed by Western blot. p53 is a key suppressor of tumor regulators in the apoptotic process and possesses pro-apoptotic activity through modulation of the BCL-2 family proteins that control the mitochondrial membrane permeability. As shown in Fig. 5C, 24 h treatment of HepG2 cells with 1 μM of organotin(IV) compound, caused threefold increase of p53 levels. These findings provide evidence that the cytotoxicity of the compound is related to the induction of a p53-dependent activation of the mitochondrial pathway of apoptosis.

3.2.4. ROS generation

Since the generation of intracellular ROS may be related to mitochondrial dysfunction and induction of apoptosis in various cell types, we explored whether our organotin(IV) compound could stimulate ROS generation in HepG2 cells. As illustrated in Fig. 6, the generation of ROS, cytofluorimetrically detected by the fluorescent dye DCFH-DA, dramatically increased in tin compound-treated cells compared with that of the control group, with a clear dose-response mechanism.

4. Conclusions

Ph_3Sn(Boc-Orn-O) showed strong cytotoxic and anticancer effects. Compared to cisplatin, organotin(IV) compound exhibited much higher antiproliferative activity *in vitro* with IC_{50} values for cell growth proliferation 20–60 times larger than those of *cis*-platin toward all the investigated cancer cell lines (HepG2, HTC116 and MCF-7).

Both oxidative damage and increased concentration of intracellular calcium ions seem to be the main events contributing to triorganotin-induced apoptosis in different panels of human cancer cell lines [35] and promotion of oxidative and DNA damage in rats tributyltin has been detected [36]. There are multiple DNA damage detection and repair systems in a cell but every type of DNA damage is reported to the p53 protein and its pathway [37–39], so that p53-triggered apoptosis plays an important role in regulating cell survival. Similarly, our findings show that apoptosis triggered by our organotin(IV) compound in human hepatocarcinoma cells involves a p53-dependent activation of the mitochondrial pathway of apoptosis, ROS formation and Ca^{2+} influx in the cytosol.

Acknowledgements

Financial support by the Ministero dell'Istruzione, dell'Università e della Ricerca (MIUR), Italy, and by the Università degli Studi di Palermo, Italy, is gratefully acknowledged.

NMR spectra were provided by Centro Grandi Apparecchiature – ATeNCenter – Università di Palermo, Italy, funded by P.O.R. Sicilia 2000–2006, Misura 3.15 Quota Regionale.

References

[1] M. Gielen, M. Biesemans, R. Willem, Appl. Organomet. Chem. 1 (2005) 143–155.
[2] F. Arjmand, S. Parveen, S. Tabassum, C. Pettinari, Inorg. Chim. Acta 423 (2014) 26–37.
[3] L. Pellerito, L. Nagy, Coord. Chem. Rev. 224 (2002) 111–150.
[4] M. Nath, S. Pokharia, X. Song, G. Eng, M. Gielen, M. Kemmer, M. Biesemans, R. Willem, D. de Vos, Appl. Organomet. Chem. 17 (2003) 305–314.
[5] A. Alama, B. Tasso, F. Novelli, F. Sparatore, Drug Discovery Today 14 (2009) 500–508.
[6] L. Niu, Y. Li, Q. Li, Inorg. Chim. Acta 423 (2014) 2–13.
[7] T.S. Basu Baul, A. Paul, L. Pellerito, M. Scopelliti, A. Duthie, J. Inorg. Biochem. 107 (2012) 119–128.
[8] A. Pagliarani, S. Nesci, V. Ventrella, Toxicol. In Vitro 27 (2013) 978–990.
[9] J. Brtko, Z. Dvorak, Toxicol. Lett. 234 (2015) 50–58.
[10] S.K. Hadjikakou, N. Hadjiliadis, Coord. Chem. Rev. 253 (2009) 235–249.
[11] M.K. Amir, S. Khan, A. Zia-ur-Rehman, I.S. Shah, Butler, Inorg. Chim. Acta 423 (2014) 14–25.
[12] G.N. Kaluđerović, H. Kommera, E. Hey-Hawkins, R. Paschke, S. Gómez-Ruiz, Metallomics 2 (2010) 419–428.
[13] A. Metsios, I. Verginadis, Y. Simos, A. Batistatou, D. Peschos, V. Ragos, P. Vezyraki, A. Evangelou, S. Karkabounas, Eur. J. Pharm. Sci. 47 (2012) 490–496.
[14] M. Nath, S. Pokharia, S. Yadhv, Coord. Chem. Rev. 215 (2001) 99–149.
[15] N. Buzás, L. Nagy, H. Jankovics, R. Krämer, E. Kuzmann, A. Vértes, K. Burger, J. Radioanal. Nucl. Chem. 241 (1999) 313–322.
[16] C. Bruyneel, Th. Zeegers-Huyskens, J. Mol. Struct. 552 (2000) 177–185.
[17] N. Khan, Y. Farina, L.K. Mun, N.F. Rajab, N. Awang, J. Organomet. Chem. 763 (2014) 26–33.
[18] M.A. Girasolo, S. Rubino, P. Portanova, G. Calvaruso, G. Ruisi, G. Stocco, J. Organomet. Chem. 695 (2010) 609–618.
[19] M.A. Girasolo, A. Attanzio, P. Sabatino, L. Tesoriere, S. Rubino, G. Stocco, Inorg. Chim. Acta 423 (2014) 168–176.
[20] F. Denizot, R. Lang, J. Immunol. Methods 89 (2) (1986) 271–277.
[21] L. Tesoriere, A. Attanzio, M. Allegra, C. Gentile, M.A. Livrea, Br. J. Nutr. 110 (2013) 230–240.
[22] S. Ramaswamy, M. Umadevi, R.K. Rajaram, V. Ramakrishnan, J. Raman Spectrosc. 34 (2003) 806–812.
[23] L.J. Bellamy, Amino-Acids, their hydrochlorides and salts, and amino-acids, in: The Infrared Spectra of Complex Molecules, third ed., 13, Chapman & Hall, London, 1975, pp. 263–276.
[24] G.B. Deacon, R.J. Philips, Coord. Chem. Rev. 33 (1980) 227–250.
[25] G.K. Sandhu, G. Kaur, J. Holeček, A. Lyčka, J. Organomet. Chem. 345 (1980) 51–57.
[26] T.S. Basu Baul, S. Dutta, E. Rivarola, R. Butcher, F.E. Smith, J. Organomet. Chem. 654 (2002) 100–108.
[27] R.C. Poller, J. Inorg. Nucl. Chem. 24 (1962) 593–600.
[28] D.H. Whiffen, J. Chem. Soc. (1956) 1350–1356.
[29] L. Dalla Via, O. Gia, Inorg. Chim. Acta 359 (2006) 4197–4206.
[30] J. Holeček, M. Nádvorník, K. Handlíř, A. Lyčka, J. Organomet. Chem. 241 (1983) 177–184.
[31] J. Holeček, K. Handlíř, M. Nádvorník, A. Lyčka, J. Organomet. Chem. 258 (1983) 147–153.
[32] T.P. Lockhart, W.F. Manders, Inorg. Chem. 25 (1986) 892–895.
[33] L. Kolářová, M. Holčapek, R. Jambor, L. Dostál, M. Nádvorník, A. Růžička, J. Mass Spectrom. 39 (2004) 621–629.
[34] T.S. Basu Baul, C. Masharing, S. Basu, E. Rivarola, M. Holčapek, R. Jirásko, A. Lyčka, D. de Vos, A. Linden, J. Organomet. Chem. 691 (2006) 952–965.
[35] B. Viviani, D. Rossi, S.C. Chow, P. Nicotera, Toxicol. Appl. Pharmacol. 140 (1996) 289–295.
[36] H.-G. Liu, Y. Wang, L. Lian, L.-H. Xu, Environ. Toxicol. 21 (2006) 166–171.
[37] A.J. Giaccia, M.B. Kastan, Genes Dev. 12 (1998) 2973–2983.
[38] A.V. Gudkov, E.A. Komarova, Nat. Rev. Cancer 3 (2003) 117–129.
[39] M. Oren, Cell Death Differ. 10 (2003) 431–442.